"Sifarchaeota" a novel Asgard phylum capable of polysaccharide degradation and anaerobic methylotrophy

Ibrahim F. Farag, Rui Zhao, Jennifer F. Biddle

School of Marine Science and Policy, University of Delaware, 1044 College Drive, Lewes DE 19958, USA.

Abstract

The Asgard superphylum is a deeply branching monophyletic group of Archaea, recently described as some of the closest relatives of the eukaryotic ancestor. The wide application of genomic analyses from metagenome sequencing has established six distinct phyla, whose genomes encode for diverse metabolic capacities and play important biogeochemical and ecological roles in marine sediments. Here, we describe two metagenome-assembled genomes (MAGs) recovered from deep marine sediments off Costa Rica margin, defining a novel lineage phylogenetically married to Thorarchaeota, as such we propose the name "Sifarchaeota" for this phylum. The two "Sifarchaeota" MAGs encode for an anaerobic methylotrophy pathway enabling the utilization of C1-C3 compounds (methanol and methylamines) to synthesize acetyl CoA. Also, the MAGs showed a remarkable saccharolytic capabilities compared to other Asgard lineages and encoded for diverse classes of carbohydrate active enzymes (CAZymes) targeting different mono-, di- and oligosaccharides. Comparative genomic analysis based on the full metabolic profiles of Asgard lineages revealed the close relation between "Sifarchaeota" and Odinarchaeota MAGs, which suggested a similar metabolic potentials and ecological roles. Furthermore, we identified multiple potential horizontal gene transfer (HGT) events from

23 different bacterial donors within “Sifarchaetoa” MAGs, which hypothetically expanded
24 “Sifarchaeota” capacities for substrate utilization, energy production and niche adaptation.
25

26 **Introduction**

27 Deep marine sediments are the home of multiple poorly described archaeal lineages, most
28 of which are yet uncultured (1)(2). Recently, the discovery of Asgard archaea in benthic
29 environments has generated great interest in novel lineages from marine sediments. Additionally,
30 greater attention directed towards studying Asgard archaea is also in part to understanding
31 eukaryogenesis, as this superphylum harbors the most closely related archaeal group to
32 eukaryotes and their genomes encode for multiple homologs of eukaryotic proteins (3)(4). So far,
33 there are 6 established Asgard phyla: Lokiarchaeota, Thorarchaeota, Odinarchaeota,
34 Heimdallarchaeota, Helarchaeota and Gerdarchaeota (4)(5)(6). The number of novel lineages yet
35 to be found is at this point unknown. This raises the need for more genome resolved metagenome
36 surveys to recover genomes of these archaeal lineages, decipher their metabolic capacities and
37 place them in the context of microbial ecology. Previous studies targeting the deep sediment
38 from the Costa Rica ~~(CR)~~ margin subseafloor have shown the presence of diverse archaeal
39 communities (7)(8). Among these archaeal lineages, members of Asgard superphyla were highly
40 abundant at multiple depths, making up 17% of the archaeal communities present (7)(8). In this
41 study on the Costa Rica margin subseafloor, we employ genome resolved metagenomics to
42 describe the metabolic potential of the genomes belonging to a new Asgard phylum.
43 Phylogenomic analysis placed the sequences of the new Asgard genomes as a sister clade to the
44 sequences of Thorarchaeota and we propose the name “Sifarchaeota” to describe this new
45 Asgard phylum. Comparative analysis shows distinct differences between Sifarchaeota and

46 previously reported Asgard archaea in terms of substrate utilization, energy production and niche
47 adaptation strategies. Finally, we detect multiple potential horizontal gene transfer (HGT) events
48 from different bacterial donors expanding the substrate utilization, energy production and
49 secondary metabolite production capacities of the Sifarchaeota.

50 **Methods**

51 **Sample collection**

52 Samples were collected during International Ocean Drilling Program (IODP) Expedition
53 334, Site U1379B on the Costa Rican Margin. Details on sample location and sampling
54 methodology have been previously described (7)(9). Microbiology samples (whole-round cores)
55 were collected on board and frozen immediately at -80°C. They were shipped to the Gulf Core
56 Repository (College Station, Texas) on dry ice and stored at -80°C until shipping to the Biddle lab
57 (Lewes, Delaware) on dry ice and further storage at -80°C. Metagenome sequencing data were
58 generated from four silty clay sediment horizons (2H-1, 2H-2, 2H-5A, and 2H-5B) in the depth
59 interval of 2-9 mbsf, within the sulfate reduction zone (7).

60 **DNA extraction, library construction and sequencing**

61 DNA for metagenomic sequencing was extracted from ~7 g sediment (~0.7 g sediment in
62 10 individual lysis tubes) using PowerSoil DNA Isolation Kit (Qiagen) following the
63 manufacturer's instructions, except for the following minor modification: the lysing tubes were
64 incubated in water bath of 60ºC for 15 min prior to beading beating on a MP machine at speed 6
65 for 45 seconds. The DNA extracts were iteratively eluted from the 10 spin columns into a final of
66 100 μL of double distilled H_2O for further analysis. Metagenomic libraries were prepared and
67 sequenced (150 bp paired-end) on an Illumina NextSeq 500 sequencer at the Genome Sequencing
68 & Genotype Center at the University of Delaware.

69 **Assembly and genome binning**

70 The raw sequencing data were processed with Trimmomatic v.0.36 (10) to remove Illumina
71 adapters and low quality reads ("SLIDINGWINDOW:10:25"). The quality-controlled reads from
72 the eight samples were de novo co-assembled into contigs using Megahit v.1.1.2 (11) with the k-
73 mer length varying from 27 to 117. Contigs longer than 1000 bp were automatically binned using
74 MaxBin2 (12) and Metabat2 (13), and the best quality ones were selected using DAS_Tool (14)
75 with the default parameters. The resulting MAGs were quality assessed using CheckM (15) and
76 taxonomically classified using GTDBTk v1.3.0 (16) using the default parameters. Genome bins of
77 >50% completeness were manually refined using the gbtools (17) based on the GC content,
78 taxonomic assignments, and differential coverages in different samples. Coverages of contigs in
79 each sample were determined by mapping trimmed reads onto the contigs using BBMap v.37.61
80 (18). Taxonomy of contigs were assigned according to the taxonomy of the single-copy marker
81 genes in contigs identified using a script modified from blobology (19) and classified by BLASTn.
82 SSU rRNA sequences in contigs were identified using Barrnap (Seeman 2015, Github), and
83 classified using VSEARCH with the SILVA 132 release (20) as the reference.

84 To improve the quality of the two novel Asgard archaea MAGs, we recruited quality-
85 controlled reads using BBMap from 2H-2, because the highest genome coverages of these two
86 MAGs were detected in this particular sample. The recruited reads were then re-assembled using
87 SPAdes v.3.12.0 (21) using default parameters. After removal of contigs shorter than 1 kb, the
88 resulting scaffolds were visualized and re-binned manually using gbtools (17) as described above.
89 The quality of the resulting Asgard archaea genomes were checked using CheckM v.1.0.7 (15)
90 with the "lineage_wf" option.

91

92 **Concatenated ribosomal protein phylogeny**

93 To determine the phylogenetic affiliations of the two Sifarchaeota MAGs in the Archaea
94 domain, we performed a thorough phylogenomic analysis based on the concatenation of 16
95 ribosomal proteins (L2, L3, L4, L5, L6, L14, L15, L16, L18, L22, L24, S3, S8, S10, S17, and
96 S19). Reference genomes were selected from all the major archaeal phyla (3-5 for each) included
97 in the GTDB database (22), except for the Asgard superphylum for which all available genomes
98 were included. Ribosomal protein sequences were detected in Anvi'o (23) using the respective
99 HMM profiles, aligned using MUSCLE v3.8.31(24), and concatenated. The maximum likelihood
100 phylogenetic tree was reconstructed using IQ-Tree (v1.6.6) (25) (located on the CIPRES web
101 server) (26) with VT + F + R10 as the best-fit substitution model selected by ModelFinder (27),
102 and single branch location was tested using 1000 ultrafast bootstraps and approximate Bayesian
103 computation (28). Branches with bootstrap support >80% were marked by black circles. In
104 addition to phylogenomic analysis, we also calculated the average nucleotide identity (ANI) using
105 FastANI (29) and average amino acid identity (AAI) using CompareM
106 (https://github.com/dparks1134/CompareM) with default settings between these novel Asgard
107 MAGs and other public available ones (i.e., those included in the GTDB database), to further
108 explore the novelty of these MAGs.

109 **Metabolic reconstruction**

110 Amino acid sequences encoded by the Sifarchaeota MAGs were predicted using Prodigal
111 v2.6.3 (30) applying the default parameters and using translation table 11. The resulting amino
112 acid sequences were screened using HMMsearch tool (31) against custom HMM databases (32)
113 representing the key genes for specific metabolic pathways to understand the potential metabolic
114 capacities and their ecological roles of Sifarchaeota. The presence/absence profiles of the

115 metabolic pathways and their completion levels were further assessed through querying the
116 predicted amino acids against KEGG database using BlastKoala tool (33). Carbohydrate-active
117 enzymes encoded by the Sifarchaeota MAGs were analyzed using dbCAN-fam-HMMs (v6)
118 database (34). Proteases, peptidases, and peptidase inhibitors encoded by the MAGS were detected
119 via USEARCH-ublast tool (35) against the MEROPS database v12.1(36). Finally, the predicted
120 amino acid sequences were queried against the TCDB database (37) using USEARCH-ublast tool
121 (35) to identify the potential transporters.

122 **Genome centric comparative analysis for the Asgard superphylum**

123 We compared the total metabolic profiles of Sifarchaetoa MAGs with representatives from
124 other Asgard lineages including (Odinarchaetoa, Thorarchaeota, Lokiarchaeota and
125 Heimdallarcaheota) to identify the key metabolic differences between each of the phyla within the
126 Asgard superphylum. We queried the representative MAGs of each of the Asgard lineages against
127 KOfam database (KEGG release 94.1) via KofamKOALA webtool (38) and using evalue 10^{-3}.
128 Then, the Asgard MAGs were clustered based on the presence/absence profiles of the identified
129 KOfams, shared between at least 3 genomes, using clustergrammer web-based tool (39) and
130 applying the Euclidean distance and average linkage type.

131 **Horizontal gene transfer (HGT) analysis**

132 The HGT events were detected through querying Sifarchaeota predicted amino acids
133 against KEGG database (KEGG release 94.1) via GhostKoala web interface (33). Proteins with
134 KO annotation, non-Asgard hits, and a bit score >100 were considered as potential HGT candidate
135 proteins. Then, the candidate set of proteins were queried against (nr) and UniProtKB/swissprot
136 databases and all proteins showing Asgard hits as one of the top hits were removed from any
137 further analysis. Finally, each candidate protein is aligned to reference set of proteins collected via

138 Annotree (40) using the corresponding KO entry and the HGT events were confirmed through
139 creating approximately-maximum-likelihood phylogenetic tree for each candidate protein using
140 FastTree v2.1 (41). An outline for the HGT detection pipeline is illustrated in Supplementary
141 Figure 1.
142
143 **Results**
144 **MAG construction and phylogenomic analysis**
145 We reconstructed 3 MAGs belonging to a potentially novel Asgard phylum with moderate
146 completion levels (67-80%) and very low contamination levels (0.93-1.9%) (Table 1). The
147 taxonomic affiliations of these potentially novel Asgard MAGs were tested using 16 ribosomal
148 proteins phylogenomic tree and it showed that both MAGs clustered together and formed a sister
149 lineage to MAGs belonging to the phylum Thorarchaeota (Figure 1). The phylogenetic analysis
150 using a set of 122 archaea specific marker proteins implemented in GTDB-tk confirmed that these
151 MAGs are belonging to a potentially novel Asgard archaeal lineage. To confirm the unique
152 positions of these candidate novel Asgard lineage, we calculated the average nucleotide identities
153 (AAI) and average amino acid identities (ANI) between the 3 novel Asgard MAGs and other
154 MAGs representing the other Asgard lineages including (Lokiarchaeota, Thorarchaeota,
155 Heimdallarchaeota and Odinarchaeota). On average, the 3 novel Asgard MAGs showed low AAI
156 values when compared to the other Asgard MAGs (<50%) (Supplementary Tables 1 and 2).
157 Two of the new Asgard MAGs, bins 190 and 142, showed a very high similarity with AAI
158 98.81% and ANI 99.52%, as such, we focused all our subsequent analysis on two MAGs, bins 042
159 and 142, since they were the most complete and unique MAGs in this study.
160

161 **Description of the taxa**

162 Although the two Sifarchaeota MAGs, bin042 and bin142, shared many metabolic
163 similarities, we could not describe them using one type strain due to the significant phylogenetic
164 distances between the two MAGs (Figure 1) and the genomic differences as described using ANI
165 and AAI values (Supplementary Tables 1 and 2). Therefore, we used two type strains to describe
166 the two putative Sifarchaeota lineages.

167 *Candidatus* Sifarchaeotum costaricensis **(*costaricensis* of or from Costa Rica).** Type material is
168 the genome designated as bin042 representing '*Candidatus* Sifarchaeotum costaricensis'.

169 *Candidatus* Sifarchaeotum subterraneus **(*subterraneus* latin name of subsurface).** Type material
170 is the genome designated as bin142 representing '*Candidatus* Sifarchaeotum subterraneus'.

171 Based on these genera, we further propose the name of a new Asgard phylum, the phylum
172 '*Candidatus* Sifarchaeota phylum nov.'

173 **Metabolic reconstruction of Sifarchaeota MAGs showed remarkable saccharolytic capacities**
174 **and potential anaerobic methylotrophy**

175 Previous reports showed that Asgard genomes encode for wide range of protein and fatty
176 acids degradation capacities (42). So far, most of the known Asgard genomes showed limited
177 saccharolytic capacities emphasized by their low genomic densities of CAZymes and sugar
178 transporters. However, Sifarchaeota showed high abundance and diversity of Carbohydrate Active
179 Enzymes (CAZymes) encoded by their MAGs specifically targeting sugars varying in
180 complexities from low (C1-C3) to moderate (C4-C6), including mono-, di- and oligo- saccharides
181 (Supplementary Figure 1, Supplementary Tables 3 and 5). Interestingly, CAZyme analysis
182 revealed the presence of different glycoside hydrolases (GH) families including cellulases and
183 endoglucanases (GH5 and GH9), cyclomaltodextrinase (GH13), α-glucosidase (GH63), β-1,4-

184 mannooligosaccharide phosphorylase (GH130) and β-L-arabinofuranosidase (GH142) targeting
185 cellobiose, maltose and maltooligosaccharides, alpha-glucosaccharides, glucose/mannose and
186 arabinosaccharides, respectively. We also identified dedicated sugar transporters mediating the
187 transfer of these sugars inside the Sifarchaeota cells, where the degradation and fermentation
188 processes take place (Supplementary Table 6). Metabolic reconstruction of Sifarchaeota MAGs
189 predict a general fermentative anaerobic life style with multiple anaerobic respiration capabilities
190 emphasized by the presence of incomplete reverse TCA cycle, presence of various fermentation
191 pathways capable of producing different fermentative products including acetate, acetoin and
192 butanediol under strictly anaerobic conditions as well as the potential capabilities to anaerobically
193 respire sulfate to sulfite and nitrite to ammonia. Notably, the degradation capacities for proteins,
194 peptides and amino acids as well as amino acid metabolism are limited in Sifarchaeota compared
195 to the other benthic archaea. Hence, Sifarchaeota may make up the short supply of fixed nitrogen
196 via reducing nitrite to ammonia and encoding for amidases to extract fixed nitrogen from nitrogen
197 containing amides like formamide.

198 Sifarchaeota MAGs showed the capacity to utilize various C1 compounds including formate
199 and methanol. For example, methanol is metabolized using an anaerobic methylotrophy pathway
200 previously described (8), suggesting the potential widespread distribution of this pathway among
201 benthic marine archaea to metabolize methylated compounds. This potential anaerobic
202 methylotrophic capacity was inferred via detecting incomplete methylotrophic methanogenesis
203 pathway, where the key genes encoding for the methyl coenzyme reductase complex were
204 completely absent. Besides, genes for incomplete Wood Ljundahl (WL) pathway were identified,
205 where only the genes of the carbonyl branch were present and the genes of the methyl branch were
206 completely absent. Detecting these set of genes in Sifarchaeota MAGs suggests the presence of

207 anaerobic methylotrophic capability, enabling Sifarchaeota to recycle methyl groups within
208 methanol and other methylated compounds. Then, these methyl groups are transferred to
209 tetrahydrofolate complex replacing the function of the methyl branch of WL pathway and
210 ultimately producing acetyl CoA.

211 **Comparative genomic analyses between different Asgard lineages shows diverse metabolic**
212 **features and life style patterns**

213 To understand the key metabolic differences between the Asgard lineages, we conducted a
214 comprehensive genome-centric analyses. As described in the methods section, we parsed 13
215 different MAGs (2 MAGs obtained from this study and 11 publicly available MAGs) belonging
216 to 5 different Asgard phyla (Lokiarchaeota, Thorarchaeota, Heimdallarchaeota, Odinarchaeota and
217 Sifarchaeota) against KOfam database using an HMM search tool (Supplementary Table 7. The
218 analysis output focused on two aspects (1) exploring the range of life style diversity within the
219 Asgard superphylum and (2) comparing the metabolic capabilities of different Asgard lineages.

220 Overall, the comparative analyses grouped the Asgard superphylum into 4 distinct clusters
221 based on their whole metabolic profiles. Notably, all the MAGs within the Asgard superphylum
222 suggested a similar fermentative anaerobic life styles, where the core genes for reverse TCA cycle,
223 various fermentation pathways were present as well as the absence of oxidative phosphorylation
224 and oxygen tolerance related genes. Here we describe the clusters and the features that drive their
225 clustering.

226 The **first cluster** grouped the 2 Sifarchaeota MAGs (bin42 and 142), obtained from this
227 study, with Candidatus Odinarchaetoa archaeon LCB4. Sifarchaeota MAGs shared multiple
228 metabolic similarities with the Odinarchaeota MAGs including limited amino acid and fatty acids
229 metabolic potentials, evident saccharolytic activities, emphasized by high density of CAZyme

230 encoding genes targeting different mono-, di- and oligosaccharide. Also, we could only identify
231 genes encoding for the oxidative branch of the pentose phosphate pathway, producing
232 Phosphoribosyl pyrophosphate (PRPP), which eventually channeled to the purine and pyrimidine
233 metabolic pathways to be used for nucleotide and nucleic acid biosynthesis. Also, MAGs within
234 this cluster encoded for large number of genes involved in C1 metabolism including formate,
235 methylamines and methanol. Genes encoding for formate dehydrogenase, methanol and
236 methylamine specific corrinoid protein:coenzyme M methyltransferases were present, which
237 suggest the potential capability of both lineages to utilize formate, methylamines and methanol as
238 carbon sources, respectively.

239 The **second cluster** grouped Lokiarchaeota and Thorarchaeota MAGs together. Unlike the
240 previous cluster, MAGs belonging to that cluster are characterized by their proteins and peptide
241 degrading capabilities emphasized by the presence of high number of proteases and peptidases
242 encoding genes ranging in density from (126-193 proteins/Mbs) and belonging to different
243 families of serine and metalloproteases. Unlike other Asgard groups, Thorarchaeota and
244 Lokiarchaeota showed the capacities to synthesize different amino acids including nonpolar amino
245 acids (e.g. isoleucine, leucine, valine and alanine), aromatic amino acids (e.g. tryptophan and
246 phenylalanine) via the shikimate pathway and charged amino acids (e.g. glutamate and lysine).
247 Similar to other Asgard archaea, MAGs belonging to Thor- and Loki- archaeota encoded for genes
248 mediating the metabolism of C1 compounds (e.g. formate), however, the absence of
249 methyltransferases encoding genes excluded the use methylated compounds as one of the potential
250 substrates.

251 Finally, **the third and fourth clusters** included different Heimdallarchaeota MAGs. The
252 separation between Heimdallarchaeota based on their metabolic profiles suggests the presence of

253 fundamental metabolic differences between the members of Heimdallarchaeota phylum and
254 supports the previous findings that described Heimdallarcaheota as a polyphyletic group (3)(6).
255 This raises the need for wider sampling efforts targeting Heimdallarchaeota genomes to fully
256 resolve their phylogenetic position and evolutionary history. However, in this study we grouped
257 all the Heimdallarchaeota MAGs and treated them as one phylum and designed a model that
258 highlights the difference between them and the other Asgard lineages. Notably, all
259 Heimdallarcahetoa MAGs showed the capacity to utilize proteins and short chain fatty acids as
260 carbon sources, while polysaccharide degradation was less supported. Similar to Loki- and
261 Throarchaeota MAGs, Heimdallarcahetoa MAGs encoded for high number of peptidases with
262 coding densities (110-210 proteins/Mbs) and belonging to diverse families of proteases and
263 peptidases including serine, metallo, cysteine and threonine peptidases (Supplementary Table 3).
264 Also, Heimdallarcahetoa MAGs showed the capacity to metabolize and synthesize nonpolar amino
265 acids (e.g. alanine, glycine, and threonine). Among all the Asgard MAGs included in this analysis,
266 only Heimdallarchaeota MAGs encoded for enzymes mediating beta-oxidation pathway including
267 acyl CoA dehydrogenase, enoyl CoA hydratase and hydroxyacyl CoA dehydrogenase, suggesting
268 their potential to use short-chain fatty acids ~~(SCFA)~~ as carbon and energy sources. Similar to all
269 other Asgards, Heimdallarchaeota encoded for incomplete WL pathway, which could have a role
270 in metabolizing C1 compounds like formate and formaldehyde.

271 Due to the limited access to the surrounding microbial community composition and
272 environmental conditions as well as the underrepresentation of the some of the lineages (only 1
273 MAG from Odinarchaeota), we could not assess the exact reasons for these diverse substrate
274 preferences between the Asgard phyla (e.g. polysaccharides in Sifarchaeota, proteins in Thor- and
275 Loki-archaeota and short-chain fatty acids in Heimdallarchaeota). Also, we are unable to conclude

276 at this point if these findings could be generalized for all the members within each phylum or it is
277 just limited to the lineages/MAGs included in the study.

278 **Role of horizontal gene transfers (HGT) in enhancing Sifarchaeota metabolic capacities and**
279 **niche adaptations**

280 We investigated the role of HGT in expanding the metabolic capacities, substrate
281 utilization and niche adaptation of the Sifarchaeota phylum. We traced the origin of each HGT
282 event and identified the extent of the spread of each gene within the Asgard superphylum
283 (Supplementary Figure 2). We successfully identified a total of 65 HGT events in Sifarchaeota, 12
284 (0.65% of the total proteins) and 53 (1.34% of the total proteins) events in bin042 and bin142,
285 respectively. Most likely, the majority of the identified HGT events were lineage specific (58,
286 89.2%) and only few similar events were detected in other Asgard lineages (7, 11.8%). Also, we
287 identified the potential donors for most of the horizontally transferred genes, ~90% of which were
288 of bacterial origins. The major bacterial contributors for the horizontally transferred genes were
289 Firmicutes (~30%), Chloroflexi (~15%), Proteobacteria (~13%), Cyanobacteria (5%) and other
290 bacterial lineages (~30%). Only a small fraction (~10%) of the horizontally transferred genes were
291 of archaeal origin outside of the Asgard superphylum (Figure 5 and Supplementary Table 8).

292 We classified HGT events based on the how widespread the transferred genes were among
293 the different Asgard phylum, as well as other archaeal lineages. Accordingly, the HGT events were
294 classified into lineage-specific**,** phylum-specific and domain-wide events. In the lineage specific
295 event, the closest relatives of the transferred genes were bacteria and the genes were exclusively
296 found in Sifarchaetoa MAGs and no orthologs were found in other Asgard or any other archaeal
297 phyla (e.g. butanediol dehydrogenase). In the phylum-specific event, the closest relatives of the
298 transferred genes were bacteria and the genes were found in multiple Asgard phyla (e.g. enoyl

299 CoA hydratase). In the domain wide event, the closest relatives of the transferred genes were
300 bacteria and the genes were found in different archaeal phyla (e.g. arsenate reductase *arsC*
301 thioredoxin) (Figure 5). In general, the functional annotation of the transferred genes showed that
302 these genes are involved in augmenting the Sifarchaeota metabolic repertoire. The majority of the
303 transferred genes fall within two metabolic modules: butanoate metabolism and biosynthesis of
304 secondary metabolites. In the butanoate metabolism, the majority of transferred genes were
305 encoding for butane diol dehydrogenases and glutaconate CoA-transferase subunits mediating the
306 key steps in pyruvate and acetate formation from butane diol and hydroxy glutaryl CoA,
307 respectively.

308 While the majority of the genes involved in the biosynthesis of secondary metabolites
309 were part of the porphyrin and chlorophyll metabolism and terpenoid biosynthesis (e.g.
310 anaerobic magnesium-protoporphyrin IX monomethyl ester cyclase and 1,4-dihydroxy-2-
311 naphthoate polyprenyltransferase). Interestingly, multiple genes involved in niche adaptation
312 may be acquired from the surrounding bacterial communities. These genes including
313 formamidase and MtaA/CmuA family methyltransferase which potentially enable Sifarchaeota
314 to utilize amide containing compounds and methylated compounds as nitrogen and carbon
315 sources, respectively. Also, a gene encodes for arsenate reductase was potentially acquired from
316 candidate division KSB1 bacterium, potentially allowing Sifarchaeota to use arsenate containing
317 compounds as final electron acceptors.

318 **Discussion**

319 In this study, we recovered three MAGs from deep Costa Rica sediments belonging to a new
320 Asgard phylum, forming a sister clade to MAGs belonging to Thorarchaeota. We propose the name
321 Sifarchaeota for this phylum, named after the Norse goddess, Sif, wife of Thor. Putative collective

322 metabolic profiles of the Sifarchaeota MAGs showed remarkable differences in the life style and
323 niche adaptations compared to the other Asgard members. We predict a saccharolytic,
324 fermentation-based life style with limited amino acid and fatty acid metabolism, whereas most of
325 the Asgard archaea identified before this study were known for their peptide degradation and short
326 chain fatty acid oxidation capacities (3)(5)(42). We detected genes encoding for incomplete
327 methanogenesis pathways coupled with the carbonyl branch of WL pathway suggesting the
328 capability of Sifarchaeota to perform anaerobic methylotrophy enabling the utilization of various
329 methylated compounds (e.g. methanol and methylamines). The widespread of anaerobic
330 methylotrophy in multiple benthic archaea highlights the importance of this pathway as an
331 effective strategy to utilize various methylated compounds commonly encountered in the marine
332 sediment niches (8)(43). On the other hand, Sifarchaeota MAGs shared similar potential
333 biogeochemical functions with other Asgard archaea including the presence of nitrite reductase
334 (*nirBD*) genes, putatively enabling Sifarchaeota members to reduce nitrite to ammonia as well as
335 genes encoding for sulfate adenylyltransferase (*sat*) and phosphoadenosine phosphosulfate
336 reductase (*cysH*), signifying their putative capability to perform assimilatory sulfate reduction and
337 sulfate activation. These shared characteristics between Asgard genomes confirm the significant
338 roles of different Asgard lineages in nitrogen and sulfur biogeochemical cycles in marine sediment
339 environments.

340 We also gauged the role of HGT in shaping the evolution of Sifarchaeaota. Our analysis
341 suggests that HGT events either added novel genes to the Sifarchaeota pangenome that impart new
342 functions e.g. butanoate metabolism and biosynthesis of secondary metabolites or enabled the
343 utilization of alternative non-organic compounds as electron source e.g. arsenate reductase.
344 Moreover, we explored the range of horizontally transferred gene donors and we concluded that

HGT is not limited to a specific phylogenetic group and probably acquired from the surrounding bacterial communities, normally present in deep marine sediments. Finally, 91% of HGT events are Sifarchaeota lineage specific and probably took place relatively recently during the course of evolution, after the diversification of Sifarchaeota from the other Asgard lineages. We identified only 9% of the events happened earlier to the full diversification of Sifarchaeota from other Asgards, as well as other archaeal lineages. This could be a plausible explanation for the presence of shared functions of non-archaeal origin between most of Asgard lineages.

Acknowledgements

We would like to thank the shipboard scientists and crew of IODP Expedition 334 for collecting these sediments, and the shorebased curators of the Gulf Coast Repository for their faithful stewardship of precious frozen subsurface samples. We also want to thank our high-performance computation cluster administrator, Karol Miaskiewicz, for his tireless work. This work was supported by the WM Keck Foundation award to JFB.

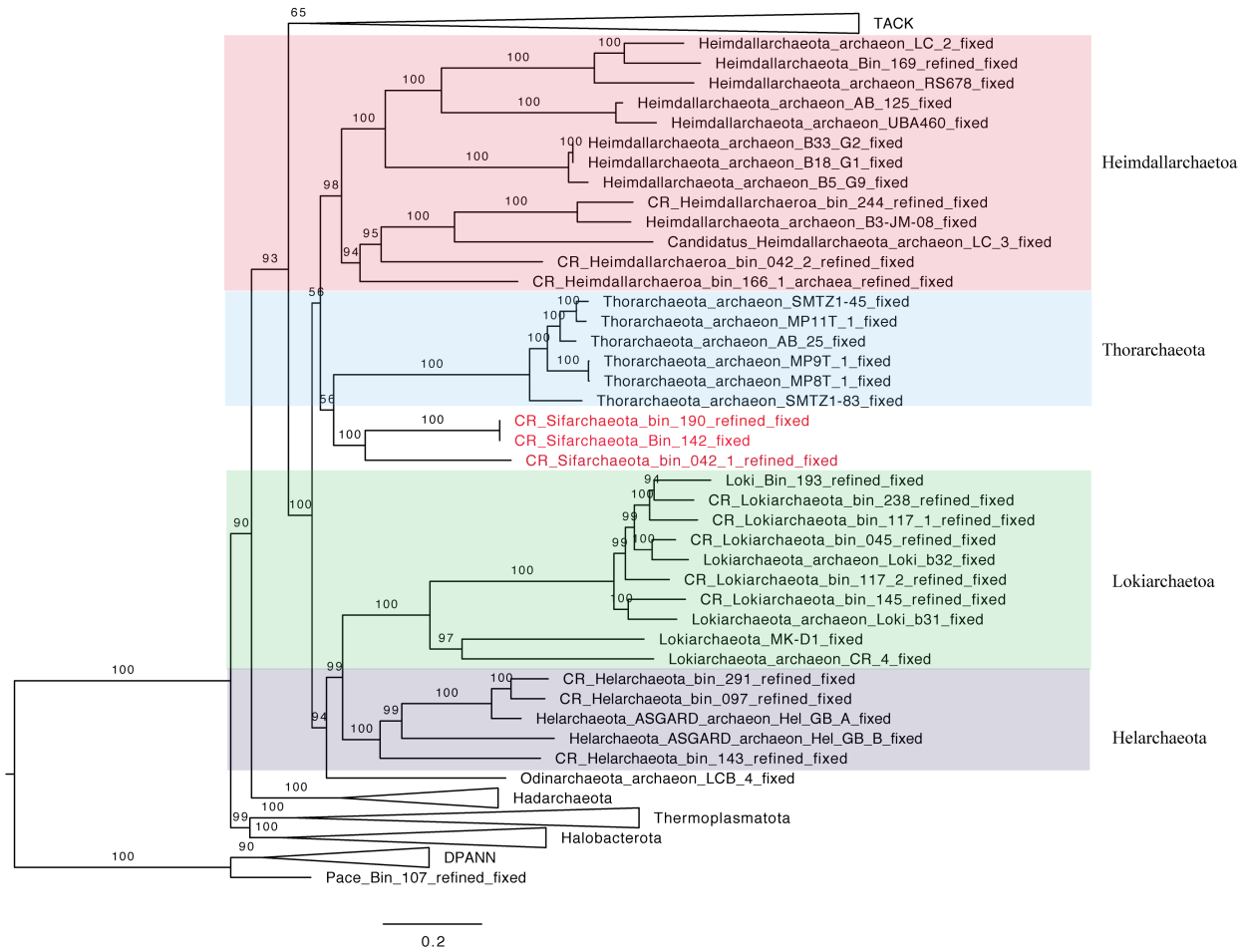

Figure 1. Maximum-likelihood phylogenetic tree of archaea genomes based on concatenated 16 ribosomal proteins. This tree was inferred using IQ-TREE v1.6.10 with the LG+R7 model and 1000 ultrafast bootstraps. The Sifarchaeota MAGs recovered in this study is highlighted in red. Lineages of the Asgard superphylum are expanded, while the other linages were collapsed, if possible. The scale bar shows estimated sequence substitutions per residue.

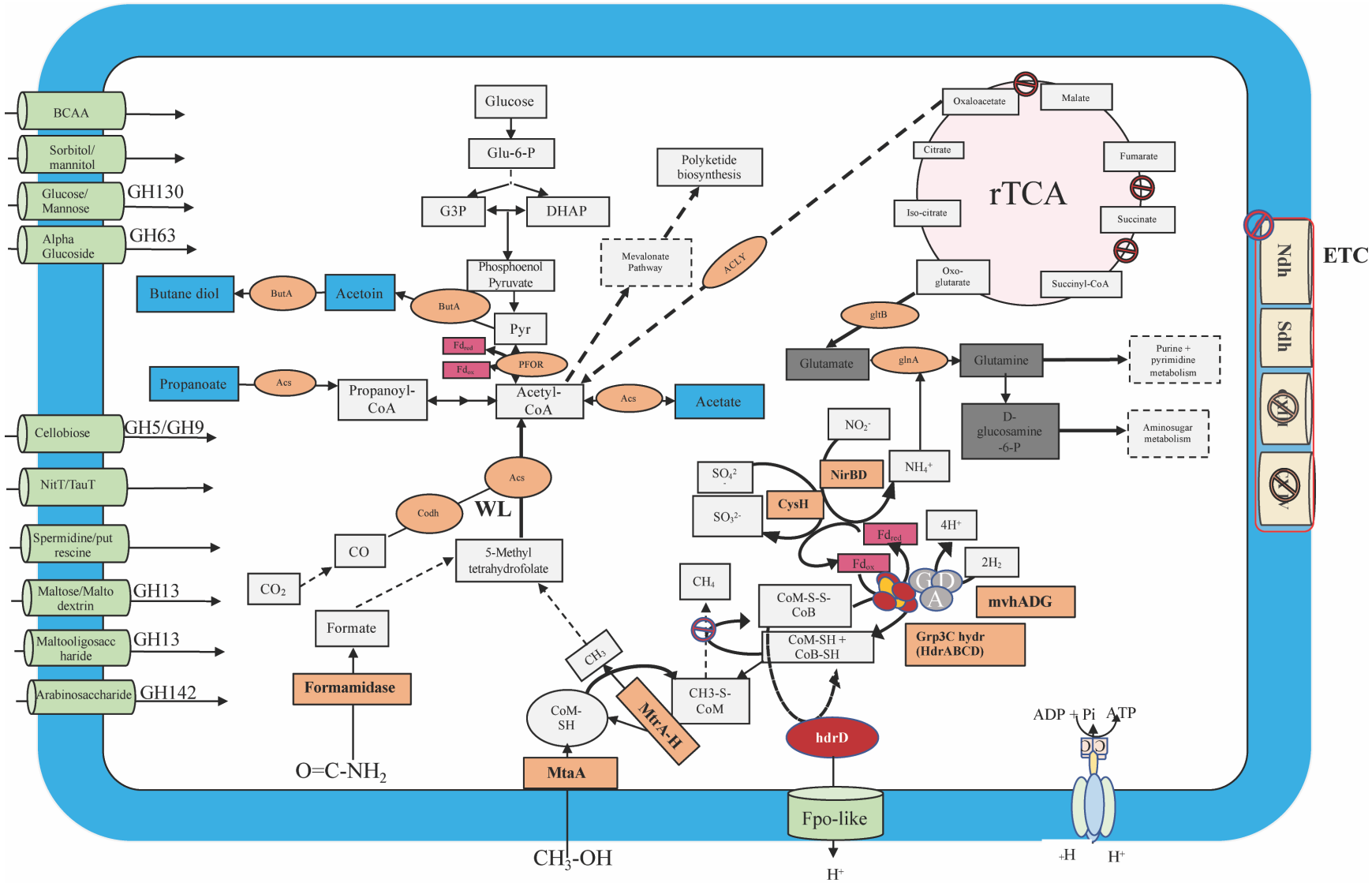
BCAA
Sorbitol/ mannitol
Glucose/ Mannose
GH130
Alpha Glucoside
GH63
Cellobiose
GH5/GH9
NitT/TauT
Spermidine/put rescine
Maltose/Malto dextrin
GH13
Maltooligosacc haride
GH13
Arabinosaccharide
GH142
Glucose
Glu-6-P
G3P
DHAP
Phosphoenol Pyruvate
Pyr
Butane diol
ButA
Acetoin
ButA
Propanoate
Acs
Propanoyl-CoA
Acetyl-CoA
Acs
Acetate
Fd red
Fd ox
PFOR
Mevalonate Pathway
Polyketide biosynthesis
ACLY
Acs
Codh
WL
CO
CO2
5-Methyl tetrahydrofolate
Formate
Formamidase
O=C-NH2
CH3
CoM-SH
MtrA-H
MtaA
CH3-OH
CH3-S-CoM
CH4
CoM-S-S-CoB
CoM-SH + CoB-SH
hdrD
Fpo-like
H+
Oxaloacetate
Malate
Citrate
Fumarate
Iso-citrate
rTCA
Succinate
Oxo-glutarate
Succinyl-CoA
gltB
Glutamate
glnA
Glutamine
Purine + pyrimidine metabolism
D-glucosamine -6-P
Aminosugar metabolism
NO2-
NH4+
NirBD
SO4 2-
SO3 2-
CysH
Fd red
Fd ox
4H+
2H2
C D A
mvhADG
Grp3C hydr (HdrABCD)
ADP + Pi
ATP
+H
H+
Ndh
Sdh
ETC

Figure 2. Metabolic reconstruction of the key metabolic pathways encoded by the Sifarchaeota MAGs. Central metabolic pathways are shown in gray boxes, carbon fixation pathways (WL and rTCA cycles) are shown in pink, electron transport chain (ETC) proteins are shown in yellow, fermentation products are shown in blue boxes, enzymes and enzyme complexes are shown in orange circles, energy carriers are shown in red, and metabolite and amino acid transporters are shown in light green.

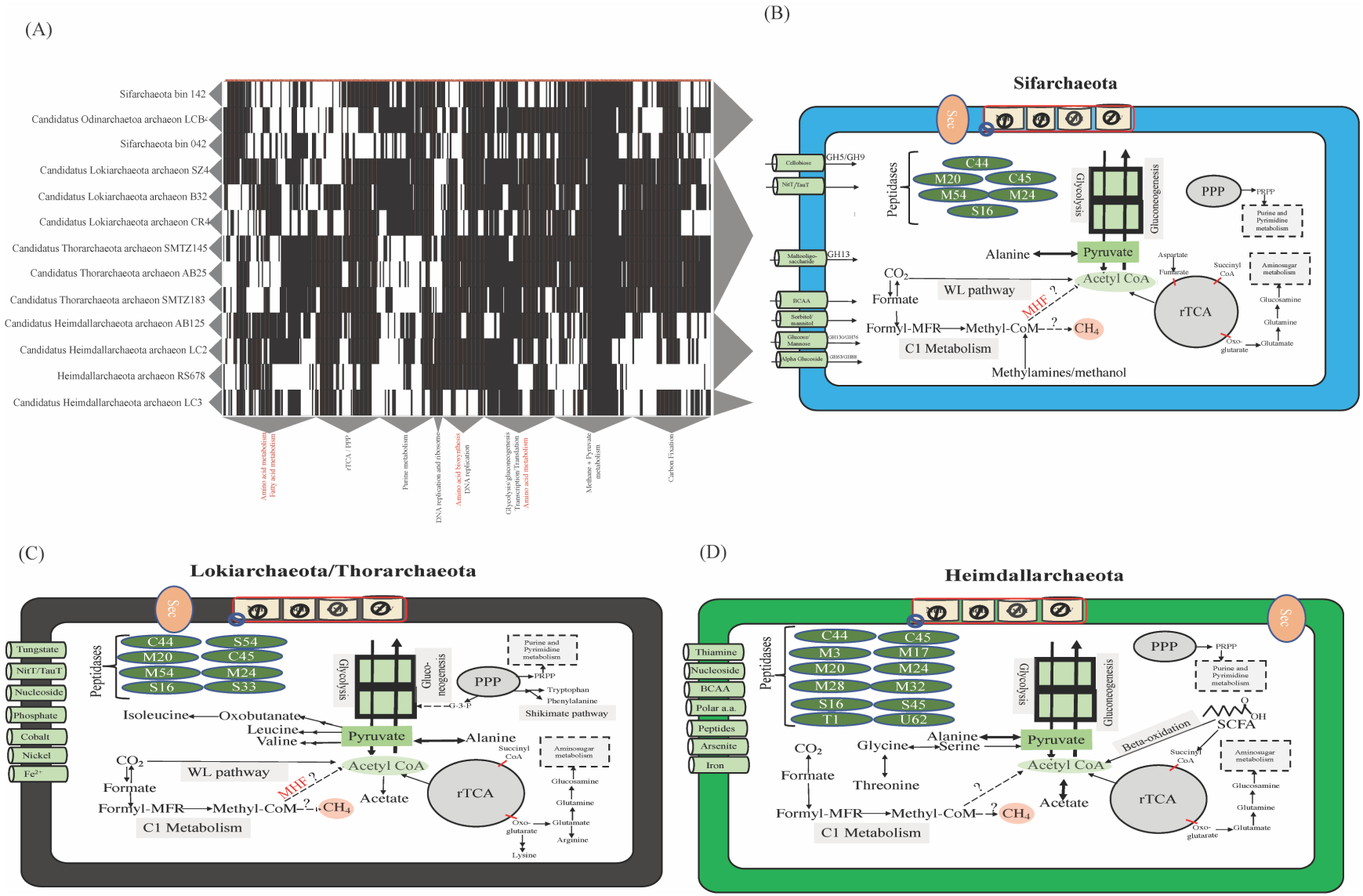
(A)
Sifarchaeota bin 142
Candidatus Odinarchaetoa archaeon LCB
Sifarchaeota bin 042
Candidatus Lokiarchaeota archaeon SZ4
Candidatus Lokiarchaeota archaeon B32
Candidatus Lokiarchaeota archaeon CR4
Candidatus Thorarchaeota archaeon SMTZ145
Candidatus Thorarchaeota archaeon AB25
Candidatus Thorarchaeota archaeon SMTZ183
Candidatus Heimdallarchaeota archaeon AB125
Candidatus Heimdallarchaeota archaeon LC2
Heimdallarchaeota archaeon RS678
Candidatus Heimdallarchaeota archaeon LC3
Amino acid metabolism
Fatty acid metabolism
rTCA / PPP
Purine metabolism
DNA replication and ribosome
Amino acid biosynthesis
DNA replication
Glycolysis/ gluconeogenesis
Transcription/Translation
Amino acid metabolism
Methane + Pyruvate metabolism
Carbon Fixation
(B)
Sifarchaeota
Sec
Cellobiose
GH5/GH9
NitT/TauT
Peptidases
C44
M20
C45
M54
M24
S16
Glycolysis
Gluconeogenesis
PPP
PRPP
Purine and Pyrimidine metabolism
Maltooligo-saccharide
GH13
Alanine
Pyruvate
Aspartate
Fumarate
Succinyl CoA
Aminosugar metabolism
CO2
Acetyl CoA
WL pathway
Formate
MHF
rTCA
Glucosamine
Glutamine
Formyl-MFR
Methyl-CoM
CH4
C1 Metabolism
Oxo-glutarate
Glutamate
BCAA
Sorbitol/ mannitol
Glucose/ Mannose
GH130/GH76
Alpha Glucoside
GH63/GH88
Methylamines/methanol
(C)
Lokiarchaeota/Thorarchaeota
Sec
Tungstate
NitT/TauT
Nucleoside
Phosphate
Cobalt
Nickel
Fe2+
Peptidases
C44
S54
M20
C45
M54
M24
S16
S33
Glycolysis
Gluco-neogenesis
PPP
Purine and Pyrimidine metabolism
PRPP
Tryptophan
Phenylalanine
Shikimate pathway
G-3-P
Isoleucine
Oxobutanate
Leucine
Valine
Pyruvate
Alanine
CO2
WL pathway
Acetyl CoA
Succinyl CoA
Aminosugar metabolism
Formate
MHF
Acetate
rTCA
Glucosamine
Glutamine
Formyl-MFR
Methyl-CoM
CH4
C1 Metabolism
Oxo-glutarate
Glutamate
Arginine
Lysine
(D)
Heimdallarchaeota
Sec
Thiamine
Nucleoside
BCAA
Polar a.a.
Peptides
Arsenite
Iron
Peptidases
C44
C45
M3
M17
M20
M24
M28
M32
S16
S45
T1
U62
Glycolysis
Gluconeogenesis
PPP
PRPP
Purine and Pyrimidine metabolism
SCFA
Beta-oxidation
Alanine
Serine
Glycine
Pyruvate
CO2
Acetyl CoA
Succinyl CoA
Aminosugar metabolism
Formate
Threonine
Acetate
rTCA
Glucosamine
Glutamine
Formyl-MFR
Methyl-CoM
CH4
C1 Metabolism
Oxo-glutarate
Glutamate

Figure 3. Comparative analysis between MAGs representing different Asgard members (A) Heatmap clustering the different Asgard MAGs (X-axis) based on their total metabolic profiles as predicted by Kofam database (Y-axis). The clustering was performed using Euclidean distance and complete linkage methods. (B) Metabolic model illustrates the key metabolic features identified in Sifarchaeota cluster. (C) Metabolic model illustrates the key metabolic features identified in Lokiarchaeota and Thorarchaeota cluster. (D) Metabolic model illustrates the key metabolic features identified in Heimdallarchaeota clusters.

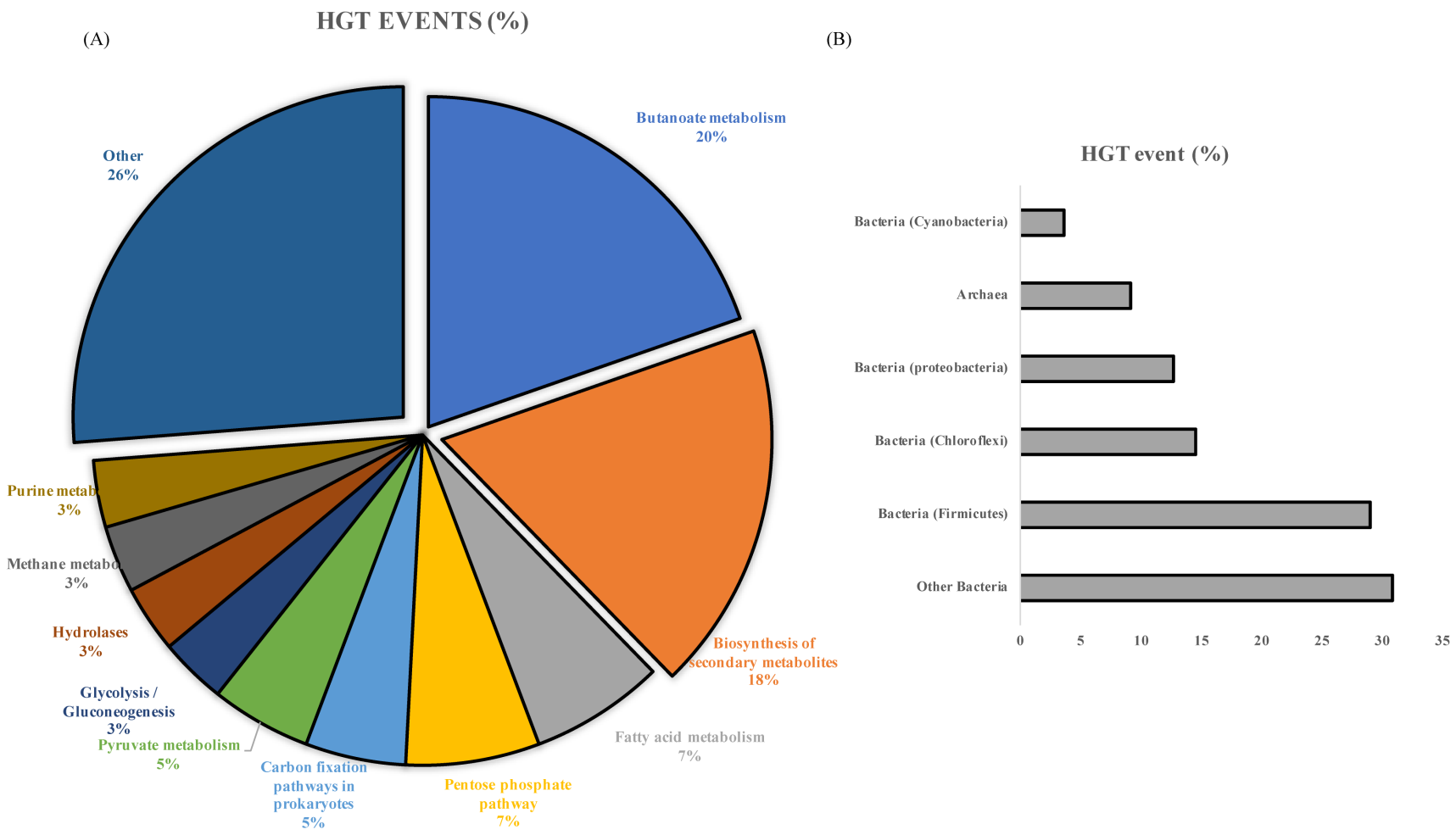

Figure 4. Summary of HGT events detected in the Sifarchaeota MAGs. (A) Different functional modules of horizontally transferred genes. (B) Major donors of the horizontally transferred genes.

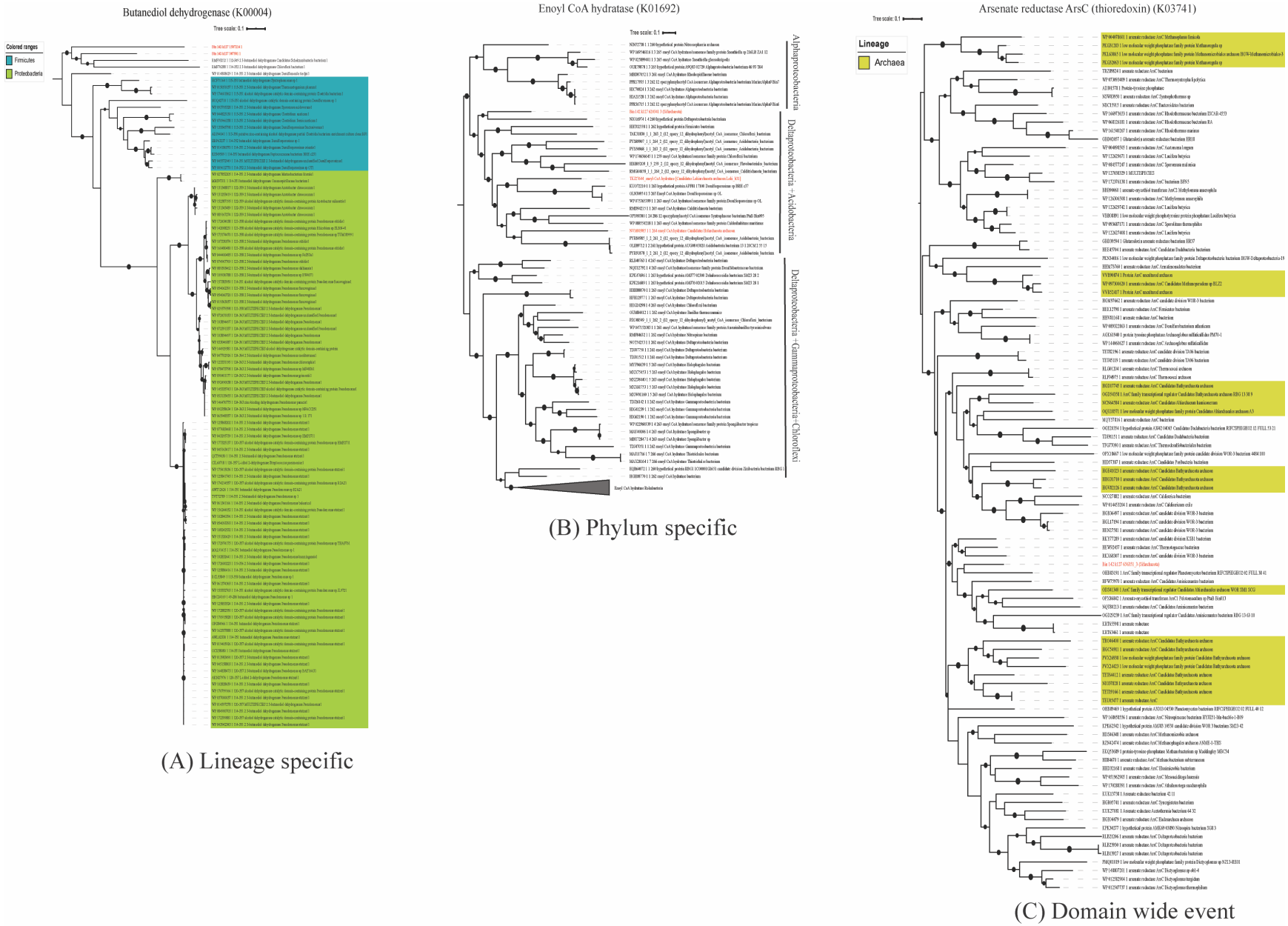
Butanediol dehydrogenase (K00004)
Tree scale: 0.1
Colored ranges
Firmicutes
Proteobacteria
(A) Lineage specific
Enoyl CoA hydratase (K01692)
Tree scale: 0.1
Alphaproteobacteria
Deltaproteobacteria
Deltaproteobacteria -Acidobacteria
Deltaproteobacteria -Gammaproteobacteria -Chloroflexi
(B) Phylum specific
Arsenate reductase ArsC (thioredoxin) (K03741)
Tree scale: 0.1
Lineage
Archaea
(C) Domain wide event

Figure 5. Examples for horizontally transferred genes in Sifarchaeota MAGs. (A) Lineage specific HGT event. Maximum likelihood phylogenetic tree of butanediol dehydrogenase gene sequences. Shaded areas correspond to the potential source organims. The tree was constructed on the basis of butanediol dehydrogenase gene sequences using FastTree. Reference sequences were obtained using AnnoTree (K00004). (B) Phylum specific HGT event. Maximum likelihood phylogenetic tree of enoyl CoA hydratase gene sequences. The tree was constructed on the basis of enoyl CoA hydratase gene sequences using FastTree. Reference sequences were obtained using AnnoTree (K01692). (C) Domain wide HGT event. Maximum likelihood phylogenetic tree of arsenate reductase ArsC thioredoxin gene sequences. The tree was constructed on the basis of arsenate reductase ArsC thioredoxin gene sequences using FastTree. Reference sequences were obtained using AnnoTree (K03741).

Table 1. Details of the Sifarchaeota MAGs analyzed in this study.

Bin ID	Completion	Contamination	Genome Size (Mbps)	Estimated Genome Size (Mbps)	Strain heterogeneity	# contigs
Bin.042_1	67.76	0.93	1.8	2.39	0	301
Bin_190	74.4	1.9	1.9	2.38	0	786
Bin_142	81.4	1.9	2.01	2.39	0	300

References

1. Teske A, Sørensen KB. 2008. Uncultured archaea in deep marine subsurface sediments: have we caught them all? ISME J 2:3–18.

2. Solden L, Lloyd K, Wrighton K. 2016. The bright side of microbial dark matter: lessons learned from the uncultivated majority. Curr Opin Microbiol 31:217–226.

3. Spang A, Saw JH, Jørgensen SL, Zaremba-Niedzwiedzka K, Martijn J, Lind AE, van Eijk R, Schleper C, Guy L, Ettema TJG. 2015. Complex archaea that bridge the gap between prokaryotes and eukaryotes. Nature 521:173–179.

4. Zaremba-Niedzwiedzka K, Caceres EF, Saw JH, Bäckström D, Juzokaite L, Vancaester E, Seitz KW, Anantharaman K, Starnawski P, Kjeldsen KU, Stott MB, Nunoura T, Banfield JF, Schramm A, Baker BJ, Spang A, Ettema TJG. 2017. Asgard archaea illuminate the origin of eukaryotic cellular complexity. Nature 541:353–358.

5. Seitz KW, Dombrowski N, Eme L, Spang A, Lombard J, Sieber JR, Teske AP, Ettema TJG, Baker BJ. 2019. Asgard archaea capable of anaerobic hydrocarbon cycling. Nat Commun 10:1822.

6. Cai M, Liu Y, Yin X, Zhou Z, Friedrich MW, Richter-Heitmann T, Nimzyk R, Kulkarni A, Wang X, Li W, Pan J, Yang Y, Gu J-D, Li M. 2020. Diverse Asgard archaea including the novel phylum Gerdarchaeota participate in organic matter degradation. Sci China Life Sci 63:886–897.

7. Amanda Martino, Matthew E. Rhodes, Rosa León-Zayas, Isabella E. Valente, Jennifer F. Biddle and Christopher H. House. 2019. Microbial Diversity in Sub-Seafloor Sediments from the Costa Rica Margin. Geosciences 9:218.

8. Farag IF, Biddle JF, Zhao R, Martino AJ, House CH, León-Zayas RI. 2020. Metabolic potentials of archaeal lineages resolved from metagenomes of deep Costa Rica sediments. ISME J 14:1345–1358.

9. Vannucchi, P.; Ujiie, K.; Stroncik, N.; IODP Exp. 334 Scientific Party; Yatheesh, V. 2013. IODP expedition 334: An investigation of the sedimentary record, fluid flow and state of stress on top of the seismogenic zone of an erosive subduction margin. Scientific Drilling vol.15:23–30.

10. Bolger AM, Lohse M, Usadel B. 2014. Trimmomatic: a flexible trimmer for Illumina sequence data. Bioinformatics 30:2114–2120.

11. Li D, Liu C-M, Luo R, Sadakane K, Lam T-W. 2015. MEGAHIT: an ultra-fast single-node solution for large and complex metagenomics assembly via succinct de Bruijn graph. Bioinformatics 31:1674–1676.

12. Wu Y-W, Tang Y-H, Tringe SG, Simmons BA, Singer SW. 2014. MaxBin: an automated binning method to recover individual genomes from metagenomes using an expectation-maximization algorithm. Microbiome 2:26.

13. Kang DD, Li F, Kirton E, Thomas A, Egan R, An H, Wang Z. 2019. MetaBAT 2: an adaptive binning algorithm for robust and efficient genome reconstruction from metagenome assemblies. PeerJ 7:e7359.

14. Sieber CMK, Probst AJ, Sharrar A, Thomas BC, Hess M, Tringe SG, Banfield JF. 2018. Recovery of genomes from metagenomes via a dereplication, aggregation and scoring strategy. Nat Microbiol 3:836–843.

15. Parks DH, Imelfort M, Skennerton CT, Hugenholtz P, Tyson GW. 2015. CheckM: assessing the quality of microbial genomes recovered from isolates, single cells, and metagenomes. Genome Res 25:1043–1055.

16. Chaumeil P-A, Mussig AJ, Hugenholtz P, Parks DH. 2019. GTDB-Tk: a toolkit to classify genomes with the Genome Taxonomy Database. Bioinformatics https://doi.org/10.1093/bioinformatics/btz848.

17. Seah BKB, Gruber-Vodicka HR. 2015. gbtools: Interactive Visualization of Metagenome Bins in R. Frontiers in Microbiology 6:1451.

18. Bushnell B. 2014. BBMap: A Fast, Accurate, Splice-Aware Aligner.

19. Kumar S, Jones M, Koutsovoulos G, Clarke M, Blaxter M. 2013. Blobology: exploring raw genome data for contaminants, symbionts and parasites using taxon-annotated GC-coverage plots. Frontiers in Genetics 4:237.

20. Quast C, Pruesse E, Yilmaz P, Gerken J, Schweer T, Yarza P, Peplies J, Glöckner FO. 2013. The SILVA ribosomal RNA gene database project: improved data processing and web-based tools. Nucleic Acids Res 41:D590-596.

21. Bankevich A, Nurk S, Antipov D, Gurevich AA, Dvorkin M, Kulikov AS, Lesin VM, Nikolenko SI, Pham S, Prjibelski AD, Pyshkin AV, Sirotkin AV, Vyahhi N, Tesler G,

Alekseyev MA, Pevzner PA. 2012. SPAdes: a new genome assembly algorithm and its applications to single-cell sequencing. J Comput Biol 19:455–477.

22. Parks DH, Chuvochina M, Waite DW, Rinke C, Skarshewski A, Chaumeil P-A, Hugenholtz P. 2018. A standardized bacterial taxonomy based on genome phylogeny substantially revises the tree of life. Nature Biotechnology 36:996–1004.

23. Eren AM, Esen ÖC, Quince C, Vineis JH, Morrison HG, Sogin ML, Delmont TO. 2015. Anvi'o: an advanced analysis and visualization platform for 'omics data. PeerJ 3:e1319.

24. Edgar RC. 2004. MUSCLE: multiple sequence alignment with high accuracy and high throughput. Nucleic Acids Res 32:1792–1797.

25. Nguyen L-T, Schmidt HA, von Haeseler A, Minh BQ. 2015. IQ-TREE: a fast and effective stochastic algorithm for estimating maximum-likelihood phylogenies. Mol Biol Evol 32:268–274.

26. Miller MA, Pfeiffer W, Schwartz T. 2010. Creating the CIPRES Science Gateway for inference of large phylogenetic trees. 2010 Gateway Computing Environments Workshop (GCE) 1–8.

27. Kalyaanamoorthy S, Minh BQ, Wong TKF, von Haeseler A, Jermiin LS. 2017. ModelFinder: fast model selection for accurate phylogenetic estimates. Nat Methods 14:587–589.

28. Hoang DT, Chernomor O, von Haeseler A, Minh BQ, Vinh LS. 2018. UFBoot2: Improving the Ultrafast Bootstrap Approximation. Mol Biol Evol 35:518–522.

29. Jain C, Rodriguez-R LM, Phillippy AM, Konstantinidis KT, Aluru S. 2018. High throughput ANI analysis of 90K prokaryotic genomes reveals clear species boundaries. Nat Commun 9:5114.

30. Hyatt D, Chen G-L, Locascio PF, Land ML, Larimer FW, Hauser LJ. 2010. Prodigal: prokaryotic gene recognition and translation initiation site identification. BMC Bioinformatics 11:119.

31. Johnson LS, Eddy SR, Portugaly E. 2010. Hidden Markov model speed heuristic and iterative HMM search procedure. BMC Bioinformatics 11:431.

32. Beckmann S, Farag IF, Zhao R, Christman GD, Prouty NG, Biddle JF. 2020. Evidence for an expanded repertoire of electron acceptors for the anaerobic oxidation of methane in authigenic carbonates in the Atlantic and Pacific Ocean. preprint, Microbiology.

33. Kanehisa M, Sato Y, Morishima K. 2016. BlastKOALA and GhostKOALA: KEGG Tools for Functional Characterization of Genome and Metagenome Sequences. J Mol Biol 428:726–731.

34. Yin Y, Mao X, Yang J, Chen X, Mao F, Xu Y. 2012. dbCAN: a web resource for automated carbohydrate-active enzyme annotation. Nucleic Acids Res 40:W445-451.

35. Edgar RC. 2010. Search and clustering orders of magnitude faster than BLAST. Bioinformatics 26:2460–2461.

36. Rawlings ND, Barrett AJ, Thomas PD, Huang X, Bateman A, Finn RD. 2018. The MEROPS database of proteolytic enzymes, their substrates and inhibitors in 2017 and a comparison with peptidases in the PANTHER database. Nucleic Acids Res 46:D624–D632.

37. Saier MH, Reddy VS, Tsu BV, Ahmed MS, Li C, Moreno-Hagelsieb G. 2016. The Transporter Classification Database (TCDB): recent advances. Nucleic Acids Res 44:D372-379.

38. Aramaki T, Blanc-Mathieu R, Endo H, Ohkubo K, Kanehisa M, Goto S, Ogata H. 2020. KofamKOALA: KEGG Ortholog assignment based on profile HMM and adaptive score threshold. Bioinformatics 36:2251–2252.

39. Fernandez NF, Gundersen GW, Rahman A, Grimes ML, Rikova K, Hornbeck P, Ma'ayan A. 2017. Clustergrammer, a web-based heatmap visualization and analysis tool for high-dimensional biological data. Sci Data 4:170151.

40. Mendler K, Chen H, Parks DH, Lobb B, Hug LA, Doxey AC. 2019. AnnoTree: visualization and exploration of a functionally annotated microbial tree of life. Nucleic Acids Res 47:4442–4448.

41. Price MN, Dehal PS, Arkin AP. 2010. FastTree 2--approximately maximum-likelihood trees for large alignments. PLoS ONE 5:e9490.

42. MacLeod F, Kindler GS, Wong HL, Chen R, Burns BP. 2019. Asgard archaea: Diversity, function, and evolutionary implications in a range of microbiomes. AIMS microbiology 5:48–61.

43. Anda VD, Chen L-X, Dombrowski N, Hua Z, Jiang H-C, Banfield J, Li W-J, Baker B. 2020. Brockarchaeota, a novel archaeal lineage capable of methylotrophy. preprint, In Review.

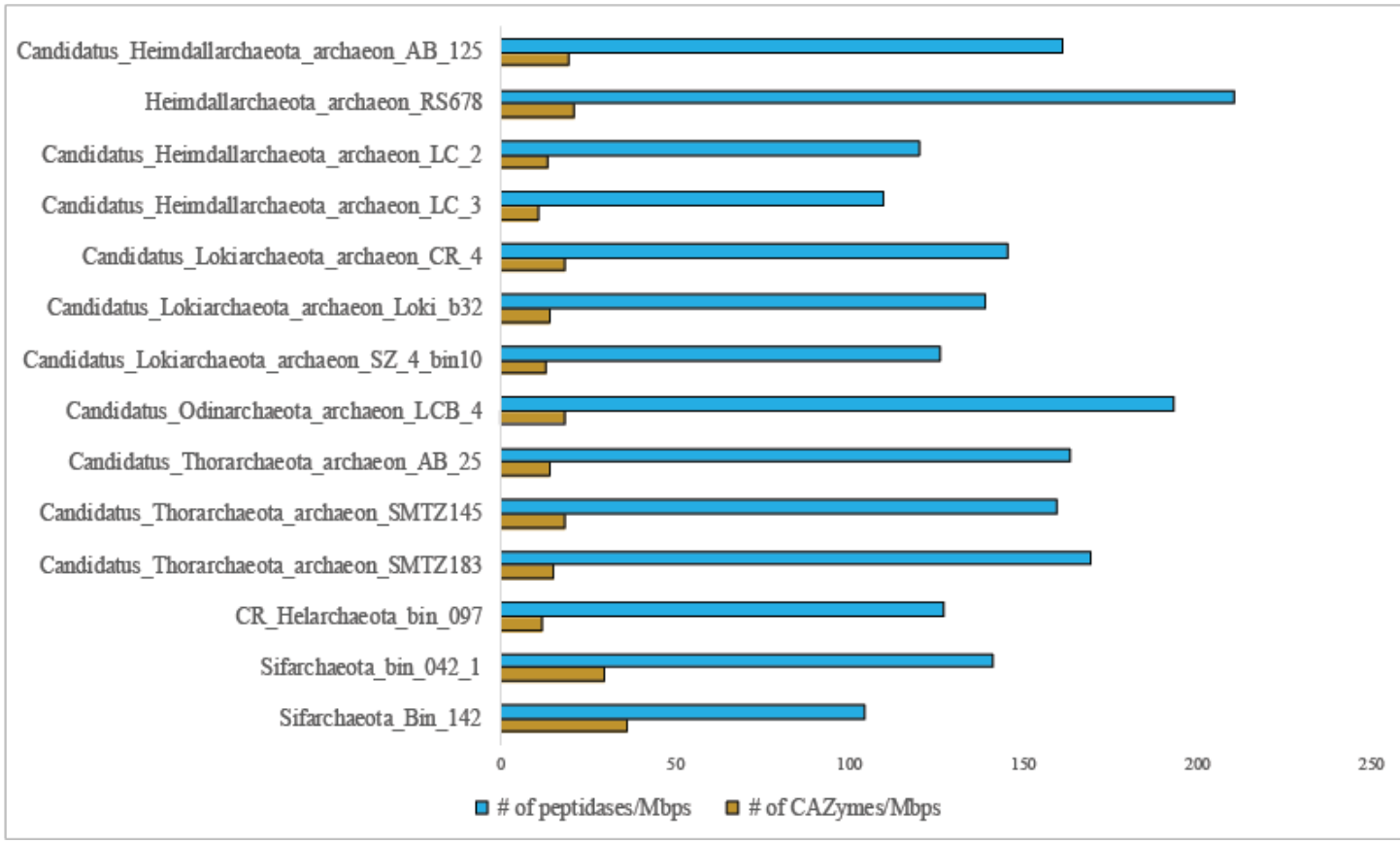

Supplementary Figure 1. Relative densities (numbers per 1 Mb) of peptidases and CAZymes encoded by the different Asgard MAGs.

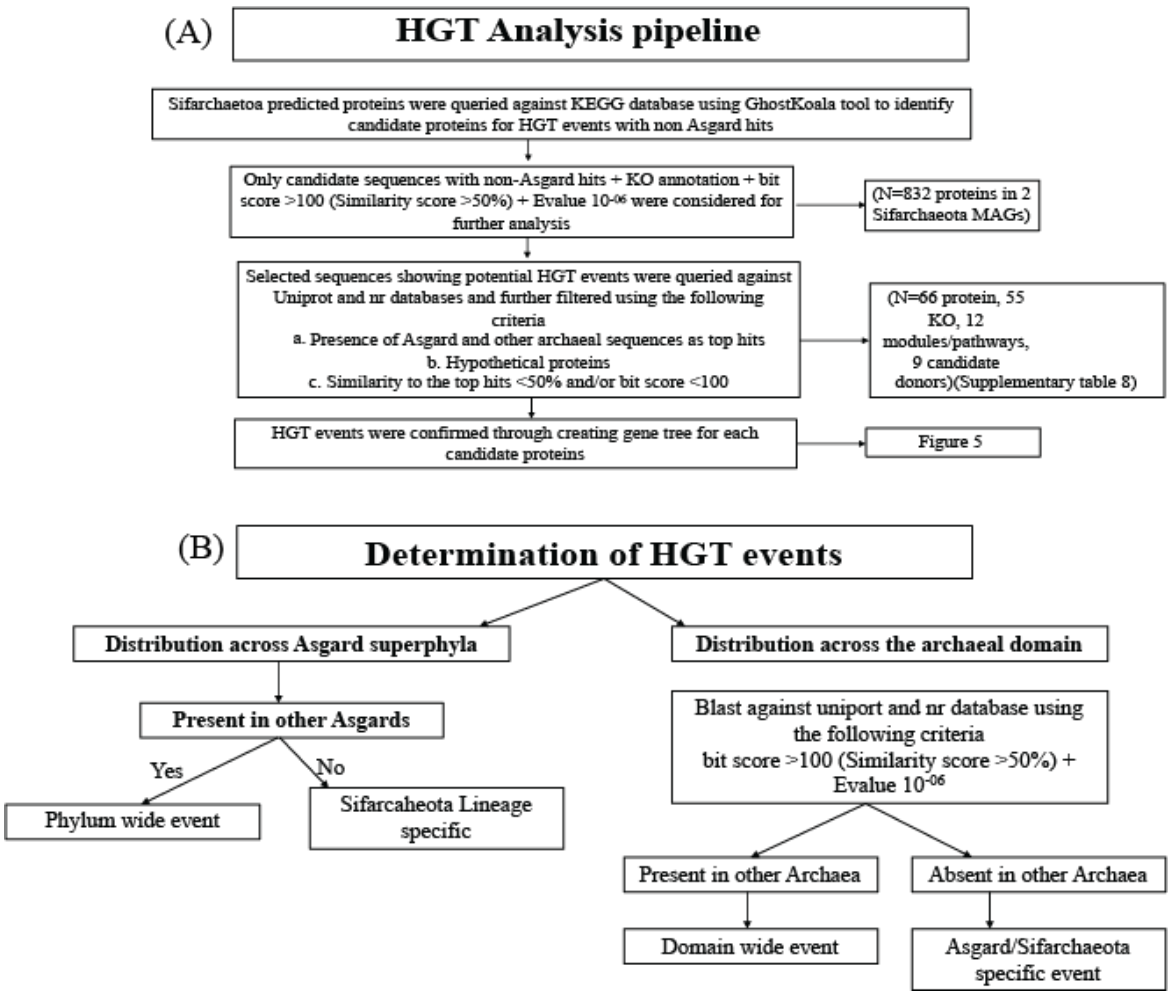

Supplementary Figure 2. Workflow diagram describes the steps followed to identify HGT events in Sifarchaeota MAGs.